

# Cyclotrons for high-intensity beams

Mike Seidel

Paul Scherrer Institute, Villigen, Switzerland

## Abstract

This paper reviews the important physical and technological aspects of cyclotrons for the acceleration of high-intensity beams. Special emphasis is given to the discussion of beam loss mechanisms and extraction schemes.

## 1 Introduction

Cyclotrons have a long history in accelerator physics and are used for a wide range of medical, industrial, and research applications [1]. The first cyclotrons were designed and built by Lawrence and Livingston [2] back in 1931. The cyclotron represents a resonant-accelerator concept with several properties that make it well suited for the acceleration of hadron beams with high average intensity. In this paper, we concentrate on aspects of the high-intensity operation of cyclotrons. The electronic version of this document contains, in the references section, clickable links to many publications related to this theme.

## 2 The classical cyclotron

Although the classical cyclotron has major limitations and is practically outdated today, some fundamental relations are best explained within this original concept. In the classical cyclotron, an alternating high voltage at radio frequency (RF) is applied to two D-shaped hollow electrodes, the *dees*, for the purpose of acceleration. Ions from a central ion source are repeatedly accelerated from one dee to the other. The ions are kept on a piecewise circular path by the application of a uniform, vertically oriented magnetic field. On the last turn, the ions are extracted by applying an electrostatic field using an electrode. The concept is illustrated in Fig. 1.

The revolution frequency of the particle motion, called the *cyclotron frequency*, depends on the magnetic field  $B_z$ , and the charge  $q$  and the effective mass  $\gamma m_0$  of the particles:

$$f_c = \frac{\omega_c}{2\pi} = \frac{qB_z}{2\pi\gamma m_0} \approx 15.2 \text{ MHz} \cdot B(\text{T}) \quad (\text{for protons}). \quad (1)$$

The frequency of the accelerating voltage must be equal to the cyclotron frequency or an integer multiple of it, i.e.,  $\omega_{\text{RF}} = h\omega_c$ . The harmonic number  $h$  equals the number of bunches that can be accelerated in one turn. With increasing velocity, particles travel at larger radii, so that  $R \propto \beta$ , and the revolution time remains constant and in phase with the RF voltage. The bending strength is given by  $B_z R \propto p \propto \beta\gamma$ . Thus, as long as  $\gamma \approx 1$ , the condition of *isochronicity* is fulfilled in a homogeneous magnetic field. However, for relativistic particles, the magnitude of the B-field has to be raised in proportion to  $\gamma$  at increasing radii, in order to keep the revolution time constant throughout the acceleration process. In summary, the condition of isochronicity in a cyclotron requires the following scaling of the orbit radius and bending field:

$$R \propto \beta, \quad B_z \propto \gamma. \quad (2)$$

This original cyclotron concept exhibits some essential properties that allow the high-intensity application of cyclotrons, which is the focus of this article. The acceleration process takes place continuously, and neither the RF frequency nor the magnetic bending field has to be cycled. The separation of subsequent turns allows continuous extraction of the beam from the cyclotron. Consequently, the production of a continuous-wave (CW) beam is a natural feature of cyclotrons. The so-called *K*-value

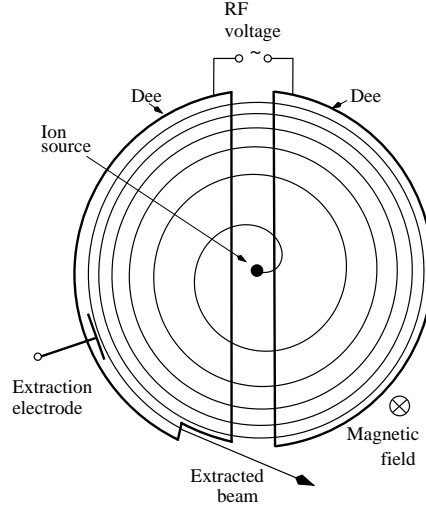


**Fig. 1:** Conceptual sketch of a classical cyclotron in plan view. In the non-relativistic approximation, the turn separation scales with the number of turns as  $n_t^{-1/2}$ .

is a commonly used parameter for the characterization of the magnetic energy reach of a cyclotron design. This equals the maximum attainable energy for protons in the non-relativistic approximation. The  $K$ -value is proportional to the maximum squared bending strength, i.e.,  $K \propto (B\rho)^2$ , and can be used to rescale the achievable kinetic energy per nucleon for varying charge-to-mass ratio:

$$\frac{E_k}{A} = K \left( \frac{Q}{A} \right)^2. \quad (3)$$

The radial variation of the bending field in a classical cyclotron generates focusing forces. At a radius  $R$ , the slope of the bending field is described by the field index  $k$ , where

$$k = \frac{R}{B_z} \frac{dB_z(R)}{dR}. \quad (4)$$

Using Eq. (2), the scaling of the field index under isochronous conditions can be evaluated as follows:

$$\begin{aligned} \frac{R}{B} \frac{dB}{dR} &= \frac{\beta}{\gamma} \frac{d\gamma}{d\beta} \\ &= \gamma^2 - 1. \end{aligned} \quad (5)$$

The radial equation of motion of a single particle can be written as

$$m\ddot{r} = mr\dot{\varphi}^2 - qr\dot{\varphi}B_z. \quad (6)$$

We now consider small deviations around the central orbit  $R$ , namely  $r = R + x$ ,  $x \ll R$ :

$$\begin{aligned} \ddot{x} + \frac{q}{m}vB_z(R+x) - \frac{v^2}{R+x} &= 0, \\ \ddot{x} + \frac{q}{m}v \left( B_z(R) + \frac{dB_z}{dR}x \right) - \frac{v^2}{R} \left( 1 - \frac{x}{R} \right) &= 0, \\ \ddot{x} + \omega_c^2(1+k)x &= 0. \end{aligned} \quad (7)$$

In this derivation, we have used the relations  $\omega_c = qB_z/m \approx v/R$  and  $r\dot{\varphi} \approx v$ . Thus, in the linear approximation, the horizontal ‘betatron motion’ is a harmonic oscillation around the central beam orbit,

$x(t) = x_{\max} \cos(\nu_r \omega_c t)$ . The parameter  $\nu_r$  is called the betatron tune. From Eq. (7), we see that the radial betatron frequency in a classical cyclotron is given by

$$\begin{aligned} \nu_r &= \sqrt{1+k} \\ &\approx \gamma. \end{aligned} \quad (8)$$

In the above, Eq. (5) has been used to derive the relation for  $\gamma$ . A similar calculation can be done for the vertical plane, using Maxwell's equation  $\text{rot } \vec{B} = 0$ . This yields the following for the vertical betatron frequency:

$$\nu_z = \sqrt{-k}. \quad (9)$$

Beta functions can be defined in the sense of the Courant–Snyder theory [3] for a cyclotron. In the radial plane, the average beta function can be estimated via

$$\beta_r \approx \frac{R}{\nu_r} \approx \frac{R}{\gamma}. \quad (10)$$

A radial dispersion function can be defined as well:

$$\Delta R = D_r \frac{\Delta p}{p}, \quad D_r \approx \frac{R}{\gamma^2}. \quad (11)$$

The derivation of this relation is done in a similar way to the calculation of the radial step width in Eq. (15) in the next section. The two relations above can be used to establish rough matching conditions for beam injection into cyclotrons. As is obvious from Eq. (9), vertical focusing can be obtained only if the bending field decreases towards larger radii. However, a negative slope of the field would be inconsistent with the isochronicity condition stated above, which requires the field to increase in proportion to  $\gamma$ . Thus the classical cyclotron is limited to relatively low energies. As we will see in the next section, vertical focusing can in fact be achieved by an azimuthal variation of the bending field.

### 3 AVF and separated-sector cyclotrons

One way to overcome the problem of insufficient vertical focusing is the introduction of azimuthally varying fields, as is done in the Thomas, or AVF, cyclotron. The principle was proposed in 1938 by L.H. Thomas [4], but it took several decades before a cyclotron based on this principle was actually built (in Delft in 1958). The variation of the vertical bending field along the flight path leads to transverse forces on the particles that can be utilized to provide suitable focusing characteristics in both of the transverse planes. In a Thomas cyclotron, the average field strength can be increased as a function of radius without losing the vertical stability. As a result, this concept allows higher energies to be achieved, for example 1 GeV for protons. In fixed-focus alternating-gradient (FFAG) rings, the same type of edge focusing plays a role as well; however, in most FFAG designs, the focusing effect of the alternating gradients is dominant. The required field variation in the cyclotron can be achieved by special shaping of the poles of a compact single magnet. The focusing can be increased by the introduction of spiral sector shapes, and sector boundaries that have tilt angles with respect to the beam orbit. With such magnet configurations, the squared vertical betatron frequency is approximately

$$\nu_z^2 \approx -k + F^2(1 + 2 \tan^2 \delta), \quad F^2 = \frac{\overline{B_z^2} - \overline{B_z}^2}{\overline{B_z}^2}. \quad (12)$$

The so-called flutter factor  $F$  equals the relative root mean square (r.m.s.) variation of the bending field around the circumference of the cyclotron. The spiral angle  $\delta$  is defined as shown in Fig. 2.

The next and most recent step in the history of cyclotron development was the introduction of separated-sector cyclotrons. Such cyclotrons have a modular structure consisting of several sector-shaped

dipole magnets and RF resonators for acceleration. The modular concept makes it possible to construct larger cyclotrons that can accommodate the bending radii of ions at higher energies.

For completeness, the synchrocyclotron, which represents another way to overcome the relativistic limit, should also be mentioned here. In the synchrocyclotron, the RF frequency is varied according to the variation in the speed of the accelerated particles. This means that pulses, i.e., trains of bunches of ions, are accelerated, which results in a drastic reduction in the average beam current that can be achieved. Historically, the synchrocyclotron was an important step in pushing the energy frontier, but this concept was superseded by the invention of the synchrotron. The sector-focused cyclotron is limited in energy, but it has retained its attractiveness for high-intensity applications owing to its advantage of CW operation. A comprehensive overview article of cyclotron concepts can be found in [1].

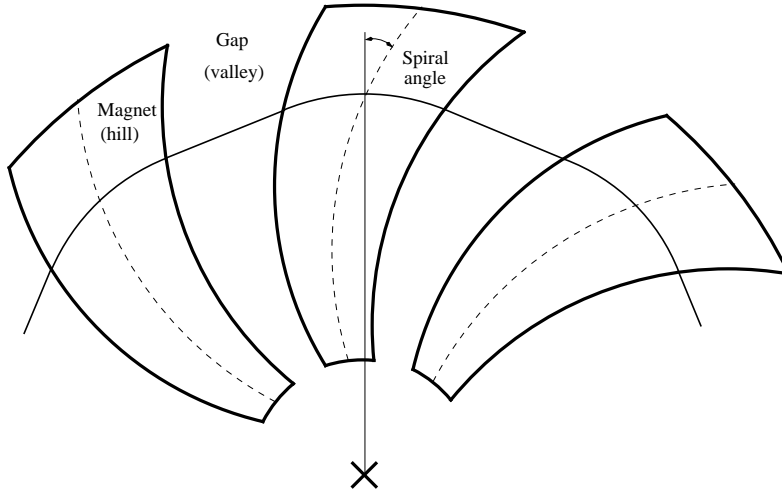


**Fig. 2:** Spiral magnet sectors and definition of the average spiral angle

For clean extraction with an extraction septum, the distance between the turns at the extraction radius must be maximized. It is therefore essential in the design of a high-intensity cyclotron to consider the transverse separation of the beam. To calculate the step width per turn, we start from the formula for the magnetic rigidity,

$$BR = \frac{p}{e} = \sqrt{\gamma^2 - 1} \frac{m_0 c}{e}. \quad (13)$$

By computing the total logarithmic differential, we obtain a relation between the changes in the radius, magnetic field, and energy of the particle beam:

$$\frac{dB}{B} + \frac{dR}{R} = \frac{\gamma d\gamma}{\gamma^2 - 1}. \quad (14)$$

Using the field index  $k$  given in Eq. (4), we obtain

$$1 + k = \frac{\gamma R}{\gamma^2 - 1} \frac{d\gamma}{dR}.$$

Noting that the change in the relativistic quantity  $\gamma$  per turn is  $d\gamma/dn_t = U_t/(m_0 c^2)$ , where  $U_t$  denotes the energy gain per turn, we finally obtain the step width in the radius,

$$\begin{aligned} \frac{dR}{dn_t} &= \frac{d\gamma}{dn_t} \frac{dR}{d\gamma} \\ &= \frac{U_t}{m_0 c^2} \frac{\gamma R}{(\gamma^2 - 1)(1 + k)} \end{aligned} \quad (15)$$

$$= \frac{U_t}{m_0 c^2} \frac{\gamma R}{(\gamma^2 - 1) \nu_r^2}. \quad (16)$$

In the outer region of the cyclotron, near the extraction radius, it is possible to violate the condition of isochronicity for a few turns. By reducing the slope of the field strength, which is related to the radial tune, it is possible to increase the turn separation locally. In the fringe field region of the magnets, the field decreases naturally. By going from Eq. (15) to Eq. (16) using Eq. (8), we can show the relation between the step width and the radial tune. If the condition of isochronicity remains valid, the dependence on the field index and the radial tune can be eliminated, and the step width is given by

$$\frac{dR}{dn_t} = \frac{U_t}{m_0 c^2} \frac{R}{(\gamma^2 - 1) \gamma}. \quad (17)$$

In this form, the equation shows the strong dependence of the step width on the beam energy. Above 1 GeV, it becomes very difficult to achieve clean extraction with an extraction septum. An effective way to increase the turn separation at the extraction element is the introduction of orbit oscillations by deliberately injecting the beam slightly off centre. When the phase and amplitude of the orbit oscillation are chosen appropriately, and also the behaviour of the radial tune is controlled in a suitable way, the beam separation can be increased by a factor of three. According to Eq. (15), this gain is equivalent to a cyclotron three times larger and is thus significant. Figure 3 illustrates how this scheme is used in the PSI Ring cyclotron. In [5], the beam profile in the outer turns was computed numerically for realistic conditions, and the results are in good agreement with measurements.

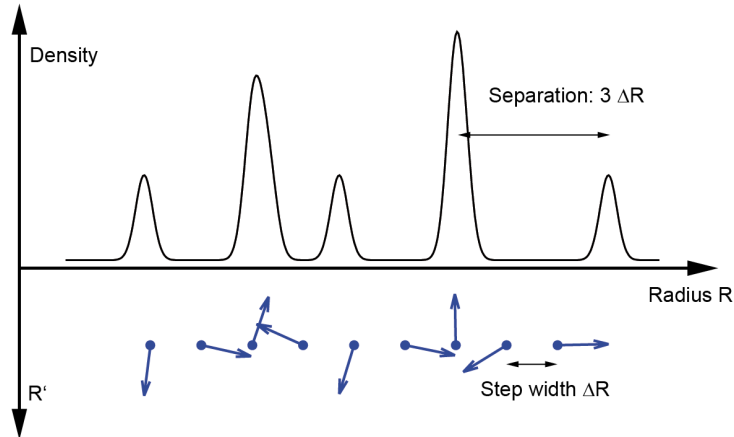


**Fig. 3:** Betatron oscillations of the centre of the beam around a closed orbit can be utilized to maximize the beam separation at extraction. The upper plot shows the calculated beam density, which is a superposition of Gaussian profiles. In the lower half, the clockwise-rotating phase space vector of the centroid of the beam is shown for each turn.

In summary, the clean extraction of the beam is of the utmost importance for high-intensity cyclotron operation. The turn separation at the extraction element can be maximized by the following measures.

- The extraction radius should be large, i.e., the overall dimensions of the cyclotron should not be chosen to be too small.
- The energy gain per turn should be maximized by installing a sufficient number of resonators with high performance.
- At relativistic energies, the turn separation diminishes quickly, and thus the final energy should be kept below approximately 1 GeV.

- In the extraction region, the turn separation can be increased by lowering the slope of the field index and by utilizing orbit oscillations resulting from controlled off-centre injection.

An alternative to the extraction method described here is extraction via charge exchange. More details of this method are given in Section 6.

#### 4 Design aspects of separated-sector cyclotrons

Modern cyclotrons that are able to reach higher  $K$ -values, particularly those designed for high intensity, are typically realized as separated-sector cyclotrons. They employ a modular concept involving a combination of sector-shaped magnets, RF resonators, and empty sector gaps to form a closed circular accelerator. The modular concept simplifies the construction of cyclotrons with diameters significantly larger than those achieved with the classical single-magnet concept. The large orbit radius at maximum energy permits extraction with extremely low losses. The modularity also has significant advantages concerning the serviceability of the accelerator, especially in view of the need to handle activated components.

During the course of acceleration, the revolution time is kept constant, which leads to a significant variation in the average orbit radius. The lateral width of the elements in the ring is large in comparison with, for example, the elements of a synchrotron that uses strong focusing. The mechanical design of the vacuum chambers and sealed interconnections is thus challenging. On the other hand, the large variation in the radius makes it possible to separate the turns at the outer radius and to realize an extraction scheme for CW operation with very low losses. The close orbit spacing in FFAG rings, for example, makes continuous extraction difficult. The extraction loss is the limiting effect for high-intensity operation of cyclotrons.

The wide vacuum chambers (2.5 m for the PSI Ring cyclotron) require special sealing techniques. In a cyclotron, as in a single-pass accelerator, vacuum levels of  $10^{-6}$  mbar are sufficient for the acceleration of protons. So-called inflatable seals are manufactured from thin steel sheets with two sealing surfaces per side and an intermittently evacuated volume between. To simplify installation, these seals are positioned on radial rails between two elements. Inflation with pressurized air seals the surfaces. This screwless scheme can tolerate small positioning errors and has the advantage of short mounting times.

The concept of the separated-sector cyclotron requires external injection of a beam of good quality. Both injection and extraction are often performed using an electrostatic deflection channel. In both cases the beam is deflected at a certain radius, while the neighbouring turns must not be affected. This is achieved by placing a thin electrode between the two turns. Particles in the beam tails that hit this electrode are scattered, and these generate losses and activation. A magnetic element would need much more material to be placed between the turns. A simplified view of the PSI Ring cyclotron is given in Fig. 4.

Some parameters of large cyclotrons operating today are listed in Table 1. The TRIUMF cyclotron [6] accelerates  $H^-$  ions and allows the extraction radius to be varied to adjust the final beam energy. The RIKEN Ring cyclotron [7] is not a high-intensity machine, but it allows a broad variety of ions to be accelerated. The special feature of the RIKEN cyclotron is the superconducting sector magnets, which deliver a very high bending strength, reflected by the corresponding  $K$ -value. The PSI Ring cyclotron was proposed in the 1960s by Willax [8]. It is specialized for high-intensity operation at the expense of reduced flexibility.

#### 5 Space charge effects in cyclotrons

In high-intensity cyclotrons, space charge effects are of major importance in determining the maximum attainable intensity. In principle, the CW operation of cyclotrons results in low bunch charges, leading to moderate space charge effects in comparison with pulsed-accelerator concepts. On the other hand, the

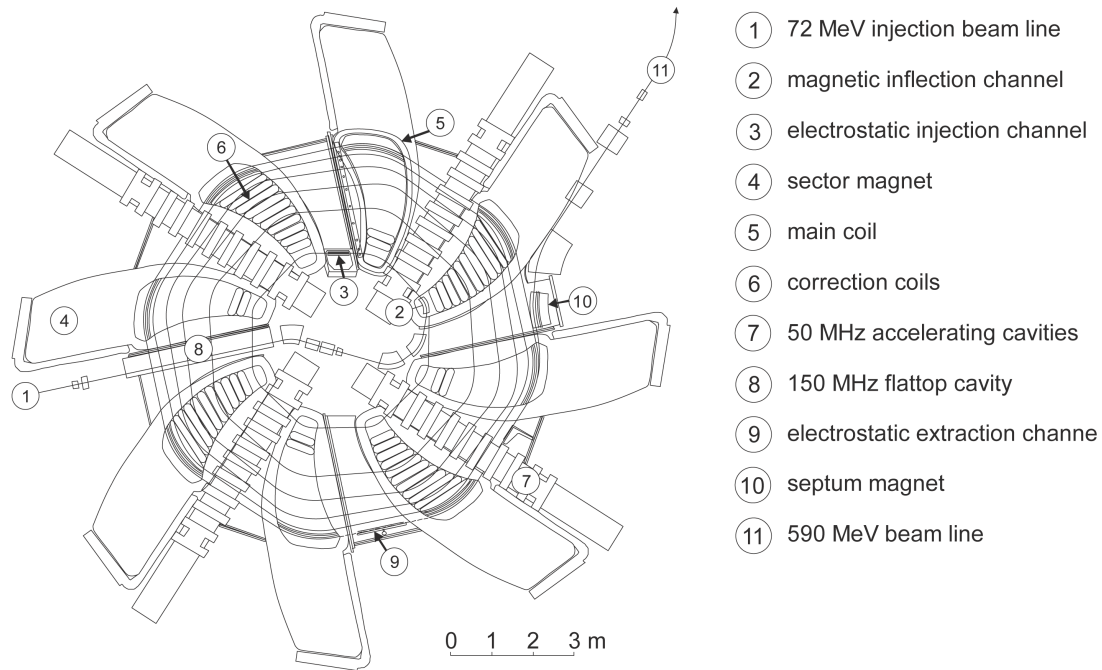


**Fig. 4:** Top view of the PSI Ring cyclotron. This separated-sector cyclotron contains eight sector magnets, four accelerating resonators (50 MHz), and one flat-top resonator (150 MHz).

**Table 1:** Selected parameters of large sector cyclotrons. The TRIUMF cyclotron uses a single magnet with sector poles. The maximum beam power of the RIKEN cyclotron was achieved in 2011, and may change with other ion species or operation modes.

Cyclotron	$K$ (MeV)	$N_{\text{mag}}$	Harmonic number	$R_{\text{inj}}$ (m)	$R_{\text{extr}}$ (m)	Extraction method	Overall transmission	$P_{\text{max}}$ (W)
TRIUMF	520	6 (sectors)	5	0.25	3.8–7.9	H <sup>-</sup> stripping channel	0.70	110
PSI Ring	592	8	6	2.1	4.5	Electrostatic channel	0.9998	1400
RIKEN Ring	2600	6	6	3.6	5.4	Electrostatic channel	0.63	6.2 ( <sup>18</sup> O)

focusing forces are rather weak. In the transverse planes, space charge forces cause shifts in the focusing frequencies, and for large tune shifts this results in resonant losses. Strong defocusing space charge forces may even exceed the focusing forces generated by the cyclotron magnets. Longitudinal space charge forces lead to an increased energy spread, which is transformed into transverse beam tails. In cyclotrons with a deflecting extraction element, these beam tails are scattered at this element and limit the intensity. Analytical prediction of the beam dynamics under the influence of space charge forces is difficult, since the beams in different turns overlap, and therefore forces from neighbouring bunches cannot be neglected in general. With particle-tracking codes, the self-induced fields of a bunch under consideration and neighbouring bunches can be included in detailed predictions of the beam dynamics [9]. However, in order to gain some insight into the fundamental dynamics, it is sufficient to consider a simplified model of uniformly charged beam sectors resulting from completely overlapping turns.

For very short transversely separated bunches, the strong repelling space charge force results in a rapid motion of the particles around the centre of the bunch on cycloidal paths. In this specific regime, a compact, stable circular bunch shape is developed, despite the presence of a repelling central force within the bunch. In this case, complete coupling between the longitudinal and radial degrees of freedom is observed. Without going into too much detail, we will briefly summarize the transverse and longitudinal effects here, as well as the formation of a round beam for short bunches.

### 5.1 Transverse space charge forces

In the case of a cyclotron with overlapping turns, a current sheet model, assuming flat rotating sectors of charge, can be applied. The vertical force on a test particle at a distance  $y$  from the beam centre is

$$F_y = \frac{n_v e^2}{\epsilon_0 \gamma^2} \cdot y. \quad (18)$$

Here,  $n_v$  is the particle density in the centre of the bunch, given by

$$n_v = \frac{N}{(2\pi)^{3/2} \sigma_y D_f R \Delta R}, \quad (19)$$

where  $D_f$  is the fraction of the circumference covered by the beam, i.e., the ratio of the average current to the peak current;  $\sigma_y$  is the vertical r.m.s. beam size;  $\Delta R$  is the step width between the turns, which was discussed in Section 3; and  $N$  is the number of particles per turn, contained in  $h$  bunches. Assuming a Gaussian longitudinal distribution with an r.m.s. bunch length  $\sigma_z$ , we have

$$D_f = \frac{h \sigma_z}{(2\pi)^{1/2} R}.$$

The focusing force generated by the magnet structure can be expressed as

$$F_y = -\gamma m_0 \omega_c^2 \nu_{y0}^2 \cdot y. \quad (20)$$

Thus the resulting vertical equation of motion for a test particle can be written as

$$\ddot{y} + \left( \omega_c^2 \nu_{y0}^2 - \frac{n e^2}{\epsilon_0 m_0 \gamma^3} \right) y = 0. \quad (21)$$

Obviously, an intensity limit is reached when the focusing term in the brackets vanishes. This condition was used by Blosser [10] to formulate a space charge limit for cyclotrons. In practice, an operating limit is reached somewhat earlier for a tune shift of approximately 0.4. The effective vertical tune can be deduced from Eq. (21) as follows:

$$\nu_y = \left( \nu_{y0} - \frac{4\pi c^2 r_p n_v}{\omega_c^2 \gamma^3} \right)^{1/2}$$



$$\approx \nu_{y0} - \frac{2\pi c^2 r_p n_v}{\omega_c^2 \gamma^3 \nu_{y0}}. \quad (22)$$

Here, the classical proton radius  $r_p = 1.5 \times 10^{-18}$  m has been introduced. After some algebra, and by replacing the step width  $\Delta R$  using Eq. (17), we finally obtain the following for the tune shift:

$$\Delta\nu_y = -\sqrt{2\pi} \frac{r_p R}{e\beta c \nu_{y0} \sigma_z} \frac{m_0 c^2}{U_t} I_{\text{avg}}. \quad (23)$$

For typical high-intensity cyclotrons, this formula predicts a space charge limit at currents of several tens of milliamps.

## 5.2 Longitudinal space charge forces

Beam losses caused by longitudinal effects are important even at the milliamp level. The effect of longitudinal space charge forces can also be estimated in a sector model. Because of the shielding effect of the vacuum chamber, only charges within a radius approximately equal to the chamber height contribute to the force. Joho [11] estimated a quadratic dependence of the accumulated energy spread on the turn number  $n_t$ :

$$\begin{aligned} \Delta E_{\text{sc}} &= \frac{16}{3} \frac{e g_{1c} Z_0}{\beta_{\text{max}}} \frac{I_{\text{avg}}}{D_f} n_t^2 \\ &\approx 2800(\Omega) \frac{e I_{\text{avg}} n_t^2}{D_f \beta_{\text{max}}}. \end{aligned} \quad (24)$$

Here,  $Z_0 = 377 \Omega$  is the impedance of free space and  $g_{1c} \approx 1.4$  is a form factor. The calculation assumes non-relativistic conditions. In Ref. [12], the results of numerical simulations were compared with this simple analytical calculation and the agreement was satisfactory.

The energy spread generated by longitudinal space charge forces is transformed into transverse beam tails. Losses occur at the electrode of the extraction element owing to residual beam density between the orbits of the last two turns. The separation between these turns is proportional to  $n_t^{-1}$ . Consequently, under the constraint of constant losses, the maximum attainable beam current scales in inverse proportion to the third power of the turn number. Over the history of the PSI cyclotron accelerator, the beam current has been increased by a large factor. This has been achieved mainly by applying higher gap voltages in the resonators, thus reducing the number of turns. More powerful RF amplifiers and new resonators have been installed. In fact, the maximum beam current scaled according to the above third-power law [14].

## 5.3 Circular-bunch regime

For very short bunches, a self-focusing effect can be observed in a cyclotron, which leads to the formation of a circular stable bunch shape in the radial-longitudinal plane. Owing to the combination of strong space charge forces and the bending dipole field, the particles start to rotate rapidly around the bunch centre in cycloidal paths. Analytical descriptions of this effect were given by Chasman and Baltz [15] for the case of a potential due to a point-like central charge and by Bertrand and Ricaud [16] for the case of a potential due to a constant charge density. The bunches in the individual turns must be separated for most of the acceleration time in order to enter the circular-shape regime. This behaviour obviously does not occur in the sector model described earlier, involving overlapping turns. A circular bunch shape is observed in practice in the Injector II cyclotron at the PSI. Figure 5 shows the measured circular particle distribution at the exit of Injector II and, for comparison, the distribution measured roughly 20 m downstream. Over the relatively short drift length, the bunch shows a significant longitudinal increase, whereas over more than 200 m travel distance in the cyclotron it stays in the compact form shown. For a high-intensity cyclotron, it is of course desirable to enter the circular-bunch regime, since the longitudinal beam blow-up can be drastically reduced.

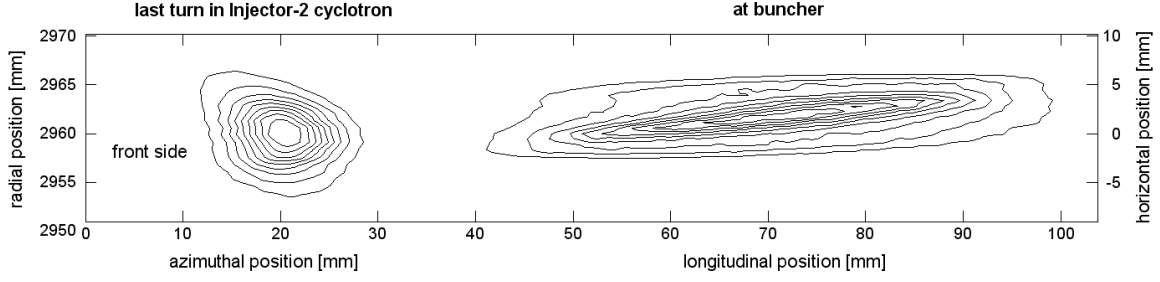


**Fig. 5:** Particle density for a current of 2.2 mA measured at the exit of the PSI Injector II cyclotron (72 MeV) and after a drift length of  $\approx 20$  m. The profile was measured by detecting protons scattered from a vertically oriented wire probe placed at varying horizontal positions. The distribution of such events was recorded as a function of time [13].

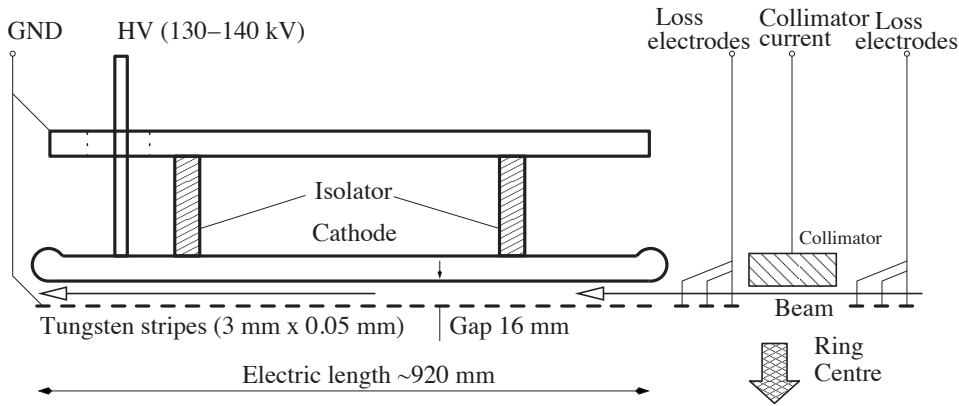


**Fig. 6:** Electrostatic extraction channel of the PSI Ring cyclotron

## 6 Injection and extraction

Extraction of the beam at high energy is one of the critical aspects of high-intensity cyclotrons. Two schemes are used for extraction. In the more classical scheme, the electrode of an electrostatic deflector is placed between the last and the second last turn in the cyclotron. The beam receives a kick angle of the order of 10 mrad, which is enough to separate the orbits to a distance that allows the insertion of a septum magnet. Although a thin electrode is typically used, some tail particles of the beam hit the electrode. The scattered particles may end up in the vacuum chamber in the extraction beam line. As described before, for this extraction scheme to work it is important to generate a large turn separation, resulting in a low beam density at the location of the electrode. A schematic drawing of an electrostatic deflector is shown in Fig. 6. The deflection angle can be calculated via the electrical rigidity,

$$E\rho = \frac{\gamma + 1}{\gamma} \frac{E_k}{q} \quad (25)$$

$$\approx 2U_{\text{gap}} \quad (\text{for } E_k \ll E_0).$$

In the low-energy approximation,  $U_{\text{gap}}$  denotes the gap voltage of the electrostatic deflector.

The other extraction scheme utilizes a stripping foil at the extraction point. Accelerated ions change their charge state when they pass through the foil. Owing to the change in the curvature of the orbit, the beam can then be extracted from the cyclotron bending field. This scheme can be applied to  $\text{H}^-$  or  $\text{H}_2^+$  ions in order to produce a proton beam. However, the second electron of the  $\text{H}^-$  ion is weakly bound, and thus there exists a significant probability that the electron will be detached from the ion in a strong magnetic field. This effect generates unwanted losses from the beam.  $\text{H}^-$  ions are accelerated

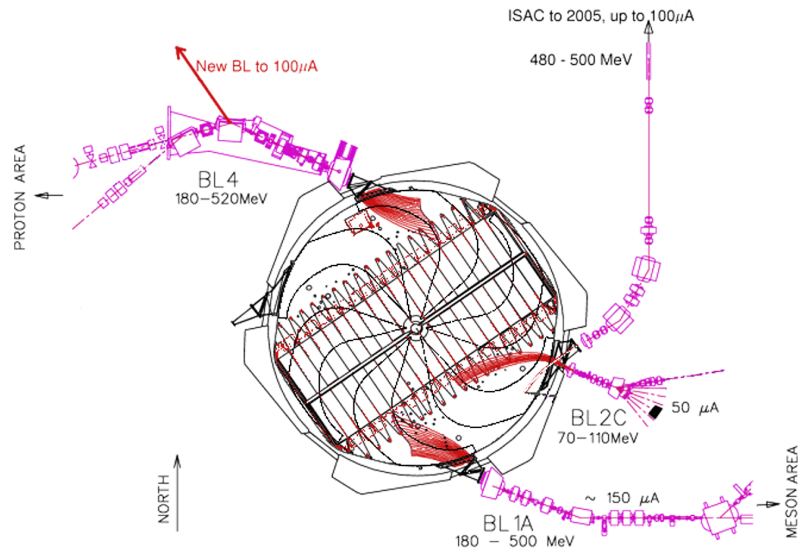


**Fig. 7:** Top view of the TRIUMF cyclotron, showing multiple extraction paths of stripped protons (drawing provided by R. Baartmann, TRIUMF, 2011)

in the TRIUMF cyclotron; this provides versatility in the form of options to extract the beam at different energies, and even at several extraction points in parallel (Fig. 7). To limit the losses from unwanted ionization, a moderate average field of 0.46 T was chosen for this cyclotron. The  $H_2^+$  ion has a stronger binding energy. However, the bending field of the cyclotron must be stronger because of the smaller charge-to-mass ratio of  $1/2$  [17].

In summary, charge stripping represents an elegant method of extracting beams from a cyclotron. However, the following effects can potentially limit the efficiency of the stripping method and must be investigated.

- Scattering from residual gas molecules, and strong magnetic fields can cause dissociation and thus loss of the accelerated ions.
- The stripping process can also generate particles with unwanted charge-to-mass ratios, for example neutrals, and the transport and the locations of loss of these particles must be considered.
- The lifetime of the stripping foil is typically problematic; the foil is heated by power deposition from the beam and also the stripped electrons, which are bound in the presence of strong magnetic fields.

## 7 Magnets

As stated previously, the condition of isochronicity in a cyclotron requires the average magnetic field to be increased in proportion to  $\gamma$  as the radius increases. The cyclotron magnets have to be designed in such a way as to fulfil this requirement. The increase in average field can be achieved by introducing a slight vertical opening angle between the magnet poles. For fine-tuning of the isochronicity, cyclotron magnets are typically equipped with several correction coil circuits. Because of the variation in the radius of the beam, which is typically significant, cyclotron magnets have to cover a wide radial range. The mechanical design becomes large and heavy. In the case of the PSI Ring cyclotron, each magnet has a weight of 280 t. A field map and a photograph of the sector magnets of the PSI Ring cyclotron are shown as an example in Fig. 8. Besides the purpose of bending the beam orbit, the magnets must provide sufficient focusing in both planes. The magnets often have a spiral shape for this purpose (see

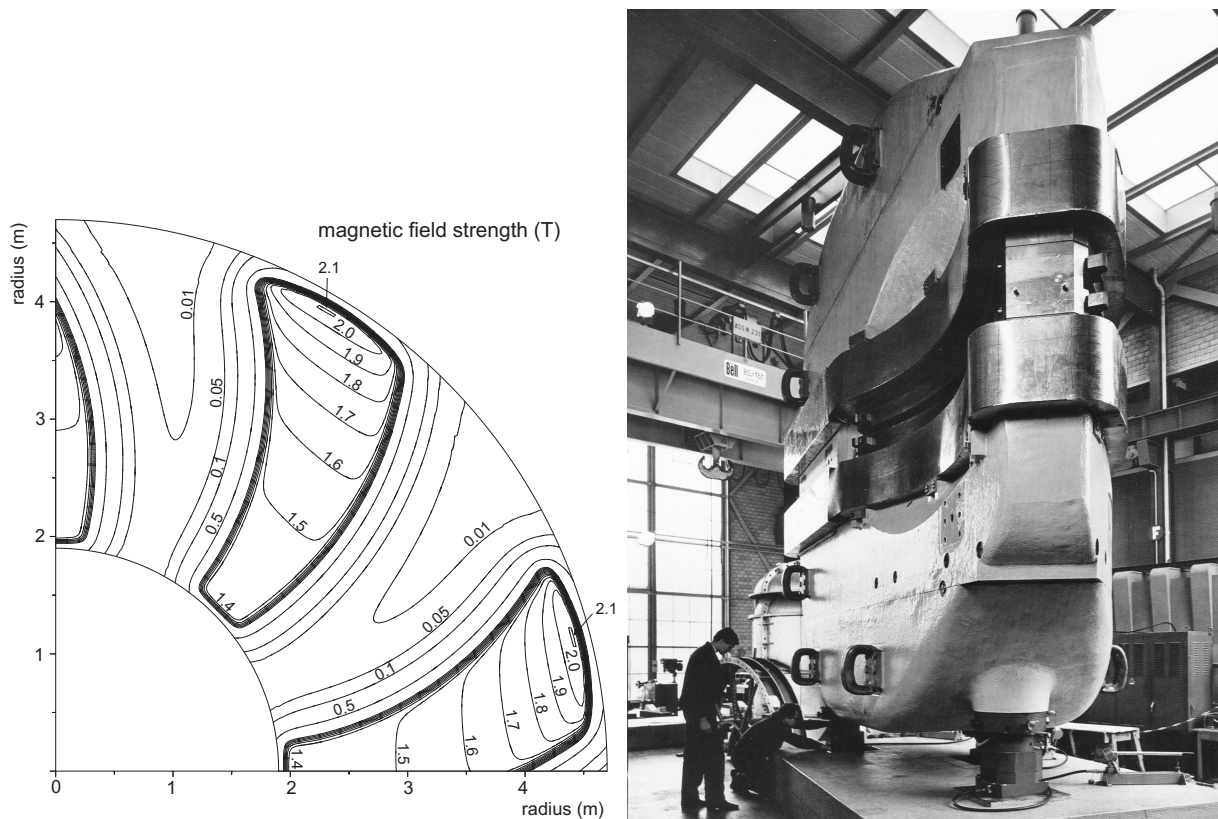


**Fig. 8:** Left: field map of the Ring cyclotron sector magnets at the PSI. The field increases towards larger radii to keep the particle revolution time constant. Right: photograph of a sector magnet before installation. Note the curved shape of the pole edges.

Section 3). Most sector magnets for cyclotrons use normal-conducting coils, although some medical and industrial cyclotrons use superconducting magnets, to allow a compact and cost-effective design. Joho [18] compared the weight statistics of normal-conducting and superconducting cyclotrons. On average, those using superconducting coils were lighter by a factor of 15. The RIKEN cyclotron is unusual in this context, and employs superconducting magnets with a peak field strength of 3.8 T [19].

## 8 Radio frequency systems

In a classical cyclotron, an alternating voltage is applied across the gap between the dees (Fig. 1). In a separated-sector cyclotron, the space between the magnets allows separate resonators to be installed. These resonators function in principle like a rectangular cavity and can provide a significantly higher gap voltage, for example 1 MV. The beam passes through the resonator via a slit in the midplane. The electric field strength varies as a sine function along the radius (Fig. 9).

In this configuration, the resonance frequency depends on the radial length  $l$  and the height  $a$  of the cavity:

$$f_0 = \frac{c}{2} \sqrt{\frac{1}{a^2} + \frac{1}{l^2}}. \quad (26)$$

Thus the frequency is independent of the azimuthal width  $b$  of the cavity. In practice, the shape of the cavity is not made exactly rectangular; instead, the azimuthal width is reduced in the midplane (Fig. 10) to minimize the travel time of the particles in the field. In the case of the PSI cyclotrons, all accelerating resonators are operated at 50.6 MHz. In the Ring cyclotron, the resonators are made from copper and achieve a quality factor of  $4.8 \times 10^4$ . At the time of writing, the typical gap voltage is 830 kV. The design

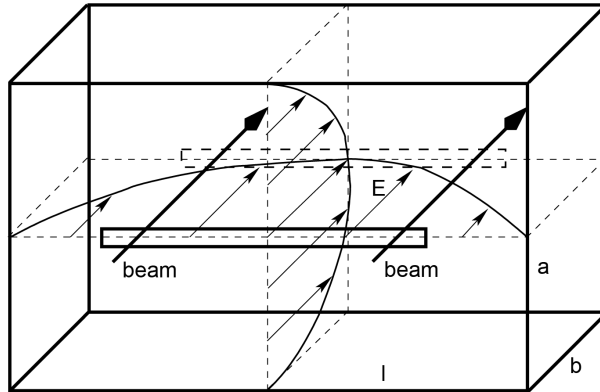


**Fig. 9:** Field distribution and orientation of the beam in a cyclotron box resonator

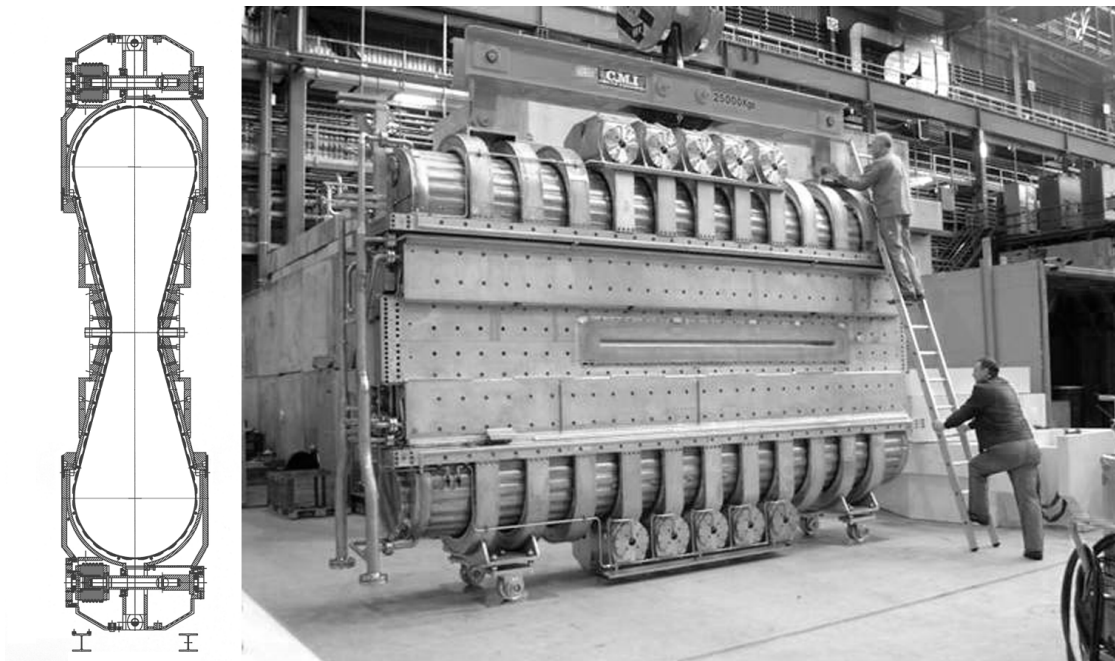


**Fig. 10:** Cross-section of PSI resonator (left), and photograph (right)

value is higher, about 1.2 MV. Each resonator can transfer 400 kW of power to the beam.

In order to minimize the variation of the energy over the bunch length, cyclotrons are often equipped with so-called flat-top resonators, which operate at the third harmonic. Using a decelerating flat-top voltage at  $1/9$  of the amplitude of the fundamental mode, the second derivative of the total voltage can be made zero at the nominal phase. In this way, the variation of the voltage as a function of the longitudinal position is minimized. For high-intensity cyclotrons, the power transfer from the electrical supply grid to the beam is a critical issue. Typically, staged tube amplifiers are used to generate the high-power RF signals required. The RF power is transferred to the resonators via coaxial lines and is coupled to the resonator volumes using loop couplers. The efficiency of the power transfer can be estimated from the product of the individual efficiencies of the components in the power transfer chain. The following values have been determined for the PSI: AC/DC conversion, 0.90; DC/RF conversion, 0.64; and RF to beam transfer, 0.55. Thus the total efficiency is about 32%, which is a relatively good number for a particle accelerator.

## 9 Performance of high-intensity cyclotrons, and discussion

As discussed in the previous sections, the major limitation on the operation of high-intensity cyclotrons is imposed by the extraction losses. With a world record beam power of 1.3 MW [20] in the PSI Ring cyclotron, the relative losses are at the level of  $10^{-4}$ . The majority of the lost protons hit the vacuum chamber in the extraction beam line and activate magnets and other accelerator components. After many years of operation, the typical activation level is around 1 mSv/h, and hotspots of approximately 10 mSv/h are observed in the extraction beam line. In order to minimize the dose to personnel during servicing of critical components, special mobile shielding devices have been developed, for example for the exchange of the electrostatic extraction channel. The ultimate criterion for the activation problem in a high-intensity accelerator is the radiation dose that the service personnel receive during maintenance work. In the PSI facility, the total charge delivered per year has significantly increased over the years. Nevertheless, there exists no correlation with the dose received by personnel [21]. This fact demonstrates that it has been possible to keep the absolute beam losses at a constant level.

Another important aspect of the performance of a high-intensity accelerator concerns the efficiency of the power transfer from the grid to the beam. The PSI accelerator complex consumes 10 MW in total, and the beam power amounts to 1.3 MW. The total power includes experimental facilities and many magnets that are not essential for the production of the high-power beam. If one considers only the RF systems, the overall efficiency is 32%. Remarkably, the majority of the beam power is transferred through only four resonators in the Ring cyclotron. A potential application of high-intensity proton accelerators is in accelerator-driven systems (ADSs), which are subcritical reactors for burning thorium [22] or the transmutation of nuclear waste [23]. For such applications, the reliability and trip rate (the rate of short beam interruptions) of the accelerator are of the utmost importance. The typical trip rate of the PSI accelerator in recent years has been in the range of 20–50 trips per day. Most trips are caused by electrical breakdowns due to the voltage in electrostatic elements. After a trip, the beam current is ramped back up to its nominal value within 30 s. Trips of the RF systems occur much less frequently. A statistical analysis of trip durations has been given in Ref. [24]. ADS systems require a much lower trip rate, of the order of 0.01–0.1 trips per day. Although there exists a promising potential for improvement (see also [24]), it will be very difficult to achieve performance in this range starting from today's performance.

The following particular advantages and disadvantages of the cyclotron concept for high-intensity beam production can be stated.

- A cyclotron requires an extraction element with an electrode placed close to the beam. By comparison, an L-band superconducting linac has a large aperture, and thus it is potentially easier to achieve low losses in a linac. The electrostatic elements in cyclotrons are critical and fragile devices, causing relatively frequent beam trips and failures.
- Because of the concept of a circular accelerator, the beam dynamics in a cyclotron is more complicated, and it requires tedious tuning to achieve an optimized operational state with low losses.
- For fundamental reasons, the maximum energy of a cyclotron is limited to roughly 1 GeV.
- The edge focusing used in cyclotrons is weaker than the alternating-gradient focusing in linacs. In particular, the space charge forces in the vertical plane lead to a limitation on the maximum beam current. It is expected that maximum currents in the region of 10 mA can be achieved in sector cyclotrons [25].
- On the pro side, the circular-cyclotron concept allows the accelerating resonators to be re-used many times. The footprint of a cyclotron facility is smaller, allowing some savings with respect to the shielding and the building.
- The low-frequency resonators in a cyclotron are robust, simple devices with low trip rates and allow very high power throughput in the couplers.
- The efficiency of the power transfer from the grid to the beam is comparatively high, in the region of 30%.

In summary, the cyclotron concept is capable of delivering high-intensity beams with a beam power of up to 10 MW and an energy of 1 GeV and represents an effective alternative to other concepts in this range.

## References

- [1] L.M. Onishchenko, *Phys. Part. Nuclei* **39** (2008) 950.
- [2] E.O. Lawrence and N.E. Edlefsen, *Science* **72** (1930) 376.
- [3] E.D. Courant and H.S. Snyder, *Ann. Phys.* **3** (1958) 1.
- [4] L.H. Thomas, *Phys. Rev.* **54** (1938) 580–598.
- [5] Y.J. Bi *et al.*, *Phys. Rev. Spec. Top. Accel. Beams* **14** (2011) 054402.
- [6] G. Dutto *et al.*, TRIUMF high intensity cyclotron development for ISAC, Proc. 17th Int. Conf. on Cyclotrons and Their Applications, Tokyo, 2004, pp. 82–86.
- [7] M. Kase *et al.*, Present status of the RIKEN Ring cyclotron, Proc. 17th Int. Conf. on Cyclotrons and Their Applications, Tokyo, 2004, pp. 160–162.
- [8] H. Willax, Proposal for a 500 MeV isochronous cyclotron with ring magnet, Proc. Int. Conf. on Sector-Focused Cyclotrons, Geneva, 1963, p. 386.
- [9] J.J. Yang *et al.*, *Phys. Rev. Spec. Top. Accel. Beams* **13** (2010) 064201.
- [10] A. Chao and M. Tigner (Eds.), *Handbook of Accelerator Physics and Engineering* (World Scientific, Singapore, 1999), Chapter 1.6.4.
- [11] W. Joho, High intensity problems in cyclotrons, Proc. 5th Int. Conf. on Cyclotrons and Their Applications, Caen, 1981, pp. 337–347.
- [12] E. Pozdeyev, A fast code for simulation of the longitudinal space charge effect in isochronous cyclotrons, Proc. 16th Int. Conf. on Cyclotrons and Their Applications, East Lansing, MI, 1981, p. 411.
- [13] R. Dölling, Measurement of the time-structure of the 72 MeV proton beam in the PSI Injector-2 cyclotron, Proc. DIPAC2001, Grenoble, 2001, pp. 111–113.
- [14] M. Seidel and P.A. Schmelzbach, Upgrade of the PSI Cyclotron Facility to 1.8 MW, Proc. 18th Int. Conf. on Cyclotrons and Their Applications, Giardini Naxos, Italy, 2007, pp. 157–162.
- [15] C. Chasman and A.J. Baltz, *Nucl. Instrum. Methods* **219** (1984) 279.
- [16] P. Bertrand and C. Ricaud, Specific cyclotron correlations under space charge effects in the case of a spherical beam, Proc. 16th Int. Conf. on Cyclotrons and Their Applications, Caen, 2001, p. 379.
- [17] L. Calabretta *et al.*, A multi-megawatt cyclotron complex to search for CP violation in the neutrino sector, Proc. Cyclotrons and Their Applications 2010, Lanzhou, China, 2010, p. 299.
- [18] W. Joho, Modern trends in cyclotrons, CERN Accelerator School: Accelerator Physics, Aarhus, Denmark, 1986, pp. 260–290.
- [19] H. Okuno *et al.*, Magnets for the RIKEN superconducting RING cyclotron, Proc. 17th Int. Conf. on Cyclotrons and Their Applications, Tokyo, 2004, pp. 373–377.
- [20] M. Seidel *et al.*, Production of a 1.3 MW proton beam at PSI, Proc. IPAC'10, Kyoto, 2010.
- [21] M. Seidel, J. Grillenberger, and A. Mezger, Experience with the production of a 1.3 MW proton beam in a cyclotron based facility, Proc. TCADS, Karlsruhe, 2010, pp. 251–260.
- [22] C. Rubbia *et al.*, An energy amplifier for cleaner and inexhaustible nuclear energy production driven by a particle beam accelerator, CERN/AT/93-47 (ET) (1993).
- [23] R. Sheffield, Utilization of accelerators for transmutation and energy production, Proc. HB2010, Morschach, Switzerland, 2010, pp. 1–5.
- [24] M. Seidel and A.C. Mezger, Performance of the PSI high power proton accelerator, IAEA, Int.

Topical Meeting on Nuclear Research Applications and Utilization of Accelerators, Vienna, 2009, AT/RD-10.

[25] T. Stambach *et al.*, *Nucl. Instrum. Methods Phys. Res. B* **113** (1996) 1–7.